Comparison of the Serum Whole Molecular Composition with the Serum Metabolome to Acquire the Pathophysiological State

Inês Correia, Tiago A. H. Fonseca, Jéssica Pataco, Mafalda Oliveira, Viviana Caldeira, N. Domingues, Cristiana P. Von Rekowski, Rúben Araújo, Luís Bento and Cecília R.C. Calado

Abstract **-** Omics Sciences serve as an essential tool to advance precision medicine. Since conventional omics sciences rely on laborious, complex and time-consuming analytical processes, this study evaluated whether the serum molecular fingerprint, captured by FTIR spectroscopy, could predict mortality risk in critically ill patients. Both the whole serum and the serum metabolome (i.e., serum after removal of macromolecules) were analyzed. PCA-LDA models demonstrated strong performance in predicting patients' pathophysiological state. A significantly more accurate model for predicting the patients' pathophysiological state was achieved using the serum metabolome (94%) compared to the whole serum (81%). This is consistent with metabolomics, which provides a more direct view of the systems' functionality. These promising results highlight the importance of FTIR spectroscopy analysis of the serum metabolome, offering a rapid, cost-effective, and high-throughput method for assessing patients' pathophysiological state.

Keywords **—** Biomarkers; FTIR spectroscopy; metabolome; Intensive Care Unit.

I. Introduction

Precision medicine aims to significantly improve the efficiency of medical diagnosis and therapy by characterizing diseases at the molecular level with greater resolution [1,2]. Omics sciences are critical tools to achieve this goal by, for example, enabling a holistic search for molecular patterns in high-dimensional data that characterize pathophysiological processes [1,2]. However, omics science is typically based on expensive, complex, laborious and time-consuming analytical procedures, difficult to implement at large-scale studies [3,4]. Furthermore, the high-dimensional data retrieved from complex and non-linear biological processes is also difficult to manage, due to inherent variability of pathophysiological processes among patients [5].

Fourier Transform Infrared (FTIR) spectroscopy can partially overcome these limitations, as it allows for a rapid, cost-effective, simple, and high-throughput acquisition of the pathophysiological state data, making it more easily applicable to large-scale populations [6-8].

Since metabolomics provides the most direct insight into the functional system of all omics [3], this study compared the whole serum molecular composition with the serum metabolome, as acquired by FTIR spectroscopy, to predict the pathophysiological state of critically ill patients.

Manuscript received: October 2024.

T. Fonseca, I Correia, J Pataco, M Oliveira, V Caldeira, R. Araújo and N Domingues are from ISEL- Instituto Superior de Engenharia de Lisboa, Instituto Politécnico de Lisboa, Lisbon, Portugal;

T. Fonseca, V Caldeira and R Araújo are from: NMS- Nova Medical School, Universidade Nova de Lisboa, Lisbon, Portugal; and CHRC - Comprehensive Health Research Centre, Universidade Nova.

L. Bento is from Intensive Care Department, ULSSJ - Unidade Local de Saúde de São José, Lisbon, Portugal and from Integrated Pathophysiological Mechanisms, CHRC.

C. Calado is from ISEL and iBB-Institute for Bioengineering and Biosciences, The Associate Laboratory Institute for Health and Bioeconomy (i4HB), Instituto Superior Técnico, Universidade de Lisboa, Lisbon, Portugal.

II. Materials and Methods

A. Population

Sixteen patients admitted to the ICU of *Hospital São José*, Lisbon, were enrolled. The present study is inserted in the PREMO project, approved by the Hospital Ethics Committee. Informed consent was obtained from each patient, or their family members, for data collection before participation. Patients' clinical information was anonymized.

All patients were male and critically ill with Coronavirus 2019 disease (COVID-19), caused by the SARS-CoV-2 virus, confirmed by Polymerase Chain Reaction (PCR). Of the sixteen patients considered, eight were successfully discharged without requiring invasive mechanical ventilation (IMV). In contrast, the remaining eight patients, who were placed under IMV, did not survive.

B. Blood collection

Peripheral blood was collected in a tube without anticoagulant at the ICU, between 7 and 9 a.m., and maintained at -4ºC, between 2 to 4 hours, till centrifugation (3500 rpm for 10min in a centrifuge Mikro220T, Hettich, Tuttlingen, Germany). Serum samples were maintained at -80ºC until further analysis. Deceased patients' samples were harvested, on average, 7 days before the occurrence.

C. Whole Serum molecular fingerprint acquisition

Triplicates of 25µL of serum, pre-diluted at 1/10 in water, from each sample, were pipetted to a 96-well Si plate and subsequently dehydrated for about 3.5h in a desiccator under vacuum (Vacuubrand, ME2, Wertheim, Germany), and the corresponding FTIR spectra were acquired.

D. Serum metabolome acquisition

Triplicates of 25µL of serum were mixed with 265 µL of a solvent mixture composed of methanol, acetonitrile, and water in a ratio of 2:2:1 (v/v). The resulting mixture was vortexed and subsequently centrifuged at 18,000 × g for 15 min at 4°C

(Mixtasel centrifuge, J.P. Selecta). Supernatants were carefully collected and stored at -80°C until analysis. On the day of the analysis, 25µL of each sample were pipetted to a 96-well Si plate and subsequently dehydrated for about 3.5h, and the corresponding FTIR spectra were acquired.

E. P-FTIR spectra acquisition

Spectral data was acquired using an FTIR spectrometer (Vertex70, Bruker) equipped with an HTS-XT microplate-reader (Bruker, Billerica, MA, USA). Each spectrum represented 64 coadded scans, with a 2cm^{-1} resolution, and was collected in transmission mode, between 400 and 4000 cm^{-1}. The first well of the 96-well plate did not contain a sample and the corresponding spectrum was acquired and used as the background, according to the HTS-XT manufacturer.

F. Data Analysis

Statistical analysis concerning the patients' demographic and clinical characteristics, were based on the Student's t-test or the non-parametric Mann-Whitney U, if data was not normally distributed. These tests were conducted with the IBM SPSS Statistics software, version 27 (IBM Corp., New York, USA). Spectra were subsequently submitted to atmospheric correction followed by either baseline correction with unit vector normalization, second derivative, or second derivate with unit vector normalization. The second derivative spectra were obtained using a Savitzky–Golay filter, with second-order polynomial over a 15-point window. The impact of spectra pre-processing was evaluated using Principal Component analysis (PCA). The following predicting models were developed: PCA-Linear Discriminant Analysis (PCA-LDA) and Support Vector Machines (SVM). A 5-fold cross-validation method (80% training, 20% test size) was applied to the SVM model. Spectra pre-processing, PCA, PCA-LDA and SVM were performed using The Unscrambler® X 10.4 software (CAMO software AS, Oslo, Norway). Univariate data analysis of spectral bands among groups was conducted using the non-parametric Mann-Whitney U test, with IBM SPSS Statistics software, version 27 (IBM Corp., New York, USA).

III. Results and Discussion

The two patient groups (i.e., discharged and deceased), were statistically different concerning variables such as age and total days in ICU for an alpha of 0.05. (**Table I**).

TABLE I. DEMOGRAPHIC AND CLINICAL CHARACTERISTICS OF THE 16 PATIENTS, WITH THE P-VALUE OF THE STATISTICAL ANALYSIS COMPARING THESE TWO GROUPS.

Variable	Discharged (n=8 patients)	Deceased (n=8 patients)	*p*-value
Age (years), (median/IQR)	52.0 (43.4-62.0)	65.0 (60.5-67.8)	0.034*
Total days in ICU (days), (median/IQR)	7.0 (5.0-8.8)	12.5 (8.0-15.3)	0.005#

*Students t-test, #Mann-Whitney U.

A. Whole serum

The **Figure 1A** represents the whole serum spectra, while **Figure 1B** represents the averaged serum spectra of the patient groups (deceased and discharged). These average spectra are very similar, and consequently, the PCA score plot (**Fig. 1C**) did not reveal a clear separation between the two groups of patients.

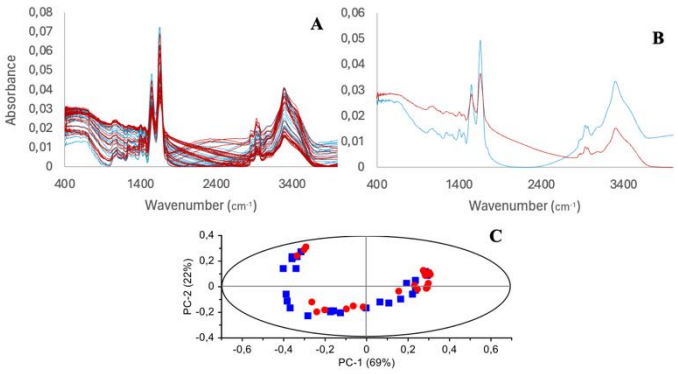

Fig. 1. FTIR spectra of the whole serum, from discharged (blue) and deceased (red) patients **(A)**. Corresponding averaged spectra **(B)** and PCA **(C)**. Data was preprocessed with atmospheric correction followed by baseline correction and normalization.

The second derivative, by enhancing the resolution of specific spectral bands, increased the differences between the two groups (**Fig. 2A**) improving the group separation in the PCA score plot (**Fig. 2B**). Despite that, data pattern separation between the two groups of patients is not clear.

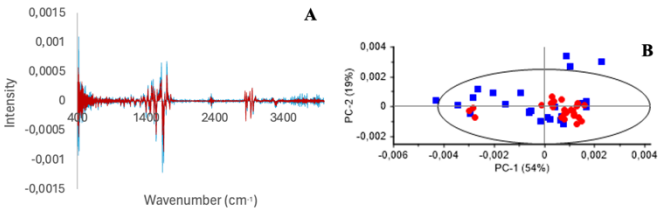

Fig. 2. The Second derivative effect on FTIR whole serum spectra in discharged (blue) and deceased (red) patients **(A)**. Corresponding PCA **(B)**.

By applying unit vector normalization to the second derivative spectra, a common scale is established, minimizing the influence of signal intensity **(Fig. 3A)**. Still, the separation pattern between the patient groups in the PCA score plot is not clear **(Fig. 3B).**

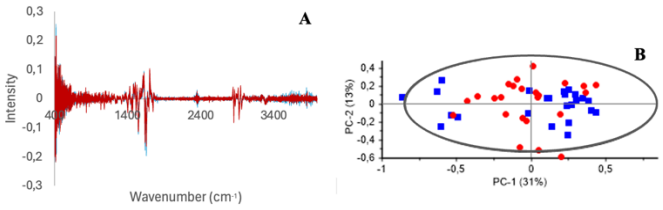

Fig. 3. The second derivative with unit vector normalization effect on whole serum spectra in discharged (blue) and deceased (red) patients **(A)**. Corresponding PCA **(B)**.

The major bands identified in the normalized baseline-corrected spectra were analyzed. An alpha level of 0.005 was set to determine statistical significance in the tests performed throughout this study. Of the 19 bands and 60 band ratios performed, 38 were statistically different between the two patient groups (**Table II**). The bands that were most significantly different between the two groups were 1056 cm^{-1} and 1077 cm^{-1}, associated with nucleic acids and glycogen, respectively. The band ratio showing the most significant difference was between 1454 cm^{-1} and 1547 cm^{-1}, associated with lipids and amide II, respectively.

The same analysis was performed on the data preprocessed with the second derivative, resulting in 37 bands and ratios that were statistically different **(Table III)**, despite a much higher number of bands and ratios being analyzed (n = 237). The band that was most significantly different between the two groups was 772 cm^{-1}. The most significant ratios were associated with phosphate groups, both from phospholipids and proteins (1080 cm^{-1}) and lipids (2927 and 2961cm^{-1}).

The analysis on the normalized second derivate spectra, resulted in the same number of statistically different bands and ratios between bands (n=37) (**Table IV**), but with smaller number of bands analyzed (n=125). In addition to the previous analysis, the most significant ratios included the amide I and II regions (1657 and 1547 cm^{-1}).

TABLE II. THE MEDIAN AND INTER-QUARTILE RANGE (IQR) OF BANDS OBTAINED FROM NORMALIZED AND BASELINE CORRECTED OF THE WHOLE SERUM SPECTRA, AND THE P-VALUE WHEN COMPARING THESE BANDS BETWEEN THE PATIENT GROUPS. ONLY BANDS WITH A P-VALUE < 0.05 ARE PRESENTED.

	Discharged		Deceased		
Bands (cm^{-1})	Median	IQR	Median	IQR	*p*-value
459	$2.68x10^{-2}$	$8.70x10^{-3}$	$2.79x10^{-2}$	$4.20x10^{-3}$	0.034
1029	$1.40x10^{-2}$	$1.53x10^{-2}$	$2.29x10^{-2}$	$9.26x10^{-3}$	0.001
1056	$1.46x10^{-2}$	$1.43x10^{-2}$	$2.31x10^{-2}$	$9.40x10^{-3}$	**<0.001**
1077	$1.48x10^{-2}$	$1.34x10^{-2}$	$2.34x10^{-2}$	$9.03x10^{-3}$	**<0.001**
1238	$1.34x10^{-2}$	$1.07x10^{-2}$	$2.07x10^{-2}$	$9.33x10^{-3}$	0.003
1314	$1.30x10^{-2}$	$9.81x10^{-3}$	$1.99x10^{-2}$	$9.24x10^{-3}$	0.006
1398	$1.62x10^{-2}$	$7.70x10^{-3}$	$2.07x10^{-2}$	$6.05x10^{-3}$	0.006
1454	$1.57x10^{-2}$	$7.51x10^{-3}$	$2.00x10^{-2}$	$5.20x10^{-3}$	0.008
1547	$3.18x10^{-2}$	$6.95x10^{-3}$	$2.91x10^{-2}$	$2.50x10^{-3}$	0.009
1660	$4.75x10^{-2}$	$1.14x10^{-2}$	$4.02x10^{-2}$	$1.05x10^{-2}$	0.008
2955	$1.44x10^{-2}$	$8.94x10^{-3}$	$8.30x10^{-3}$	$5.14x10^{-3}$	0.022
3294	$3.36x10^{-2}$	$1.76x10^{-2}$	$1.92x10^{-2}$	$1.91x10^{-2}$	0.005
3856	$3.50x10^{-3}$	$9.64x10^{-3}$	$3.42x10^{-4}$	$2.85x10^{-3}$	0.002
419/1077	$1.62x10^{0}$	$9.06x10^{-1}$	$1.23x10^{0}$	$4.49x10^{-1}$	0.008
459/1077	$1.66x10^{0}$	$9.37x10^{-1}$	$1.27x10^{0}$	$5.37x10^{-1}$	0.008
502/1077	$1.65x10^{0}$	$9.16x10^{-1}$	$1.24x10^{0}$	$6.02x10^{-1}$	0.002
619/1077	$1.61x10^{0}$	$8.54x10^{-1}$	$1.23x10^{0}$	$5.62x10^{-1}$	0.002
1547/1077	$2.15x10^{0}$	$3.35x10^{0}$	$1.23x10^{0}$	$7.20x10^{-1}$	0.001
1660/1077	$3.32x10^{0}$	$5.25x10^{0}$	$1.66x10^{0}$	$1.60x10^{0}$	0.003
619/1238	$1.77x10^{0}$	$8.25x10^{-1}$	$1.43x10^{0}$	$6.34x10^{-1}$	0.048
1547/1238	$2.43x10^{0}$	$2.59x10^{0}$	$1.41x10^{0}$	$1.00x10^{0}$	0.003
1660/1238	$3.68 x10^{0}$	$4.24x10^{0}$	$1.92x10^{0}$	$2.13x10^{0}$	0.004
1029/1547	$4.42x10^{-1}$	$5.08x10^{-1}$	$7.84x10^{-1}$	$3.30x10^{-1}$	0.002
1056/1547	$4.51x10^{-1}$	$4.90x10^{-1}$	$8.02x10^{-1}$	$3.29x10^{-1}$	0.001
1077/1547	$4.66x10^{-1}$	$4.73x10^{-1}$	$8.13x10^{-1}$	$3.19x10^{-1}$	0.001
1238/1547	$4.12x10^{-1}$	$3.82x10^{-1}$	$7.11x10^{-1}$	$3.29x10^{-1}$	0.003
1314/1547	$3.89x10^{-1}$	$3.65x10^{-1}$	$6.79x10^{-1}$	$3.25x10^{-1}$	0.003
1398/1547	$4.44x10^{-1}$	$2.93x10^{-1}$	$7.12x10^{-1}$	$2.69x10^{-1}$	0.002
1454/1547	$4.22x10^{-1}$	$2.59x10^{-1}$	$6.84x10^{-1}$	$2.50x10^{-1}$	**<0.001**
3856/1547	$9.36x10^{-2}$	$3.30x10^{-1}$	$1.03x10^{-2}$	$9.05x10^{-2}$	0.008
1029/1660	$2.85x10^{-1}$	$3.83x10^{-1}$	$5.76x10^{-1}$	$3.37x10^{-1}$	0.003
1056/1660	$2.97x10^{-1}$	$3.71x10^{-1}$	$5.92x10^{-1}$	$3.42x10^{-1}$	0.003
1077/1660	$3.02x10^{-1}$	$3.60x10^{-1}$	$6.02x10^{-1}$	$3.36x10^{-1}$	0.003
1238/1660	$2.72x10^{-1}$	$2.94x10^{-1}$	$5.23x10^{-1}$	$3.32x10^{-1}$	0.004
1314/1660	$2.57x10^{-1}$	$2.76x10^{-1}$	$4.99x10^{-1}$	$3.28x10^{-1}$	0.004
1398/1660	$2.98x10^{-1}$	$3.32x10^{-1}$	$5.23x10^{-1}$	$2.91x10^{-1}$	0.004
1454/1660	$2.88x10^{-1}$	$2.21x10^{-1}$	$5.03x10^{-1}$	$2.73x10^{-1}$	0.002
3856/1660	$6.58x10^{-2}$	$1.87x10^{-1}$	$7.48x10^{-3}$	$5.48x10^{-2}$	0.008

TABLE III. THE MEDIAN AND INTER-QUARTILE RANGE (IQR) OF BANDS OBTAINED FROM SECOND DERIVATIVE OF THE WHOLE SERUM SPECTRA, AND THE P-VALUE WHEN COMPARING THESE BANDS BETWEEN THE PATIENT GROUPS. ONLY BANDS WITH A P-VALUE < 0.05 ARE PRESENTED.

	Discharged		Deceased		
Bands (cm^{-1})	Median	IQR	Median	IQR	*p*-value
772	$-6.14x10^{-6}$	$1.71x10^{-5}$	$8.46x10^{-6}$	$1.27x10^{-5}$	**<0.001**
837	$-1.86x10^{-5}$	$1.75x10^{-5}$	$-2.72x10^{-5}$	$3.72x10^{-5}$	0.035
899	$-6.63x10^{-6}$	$1.66x10^{-5}$	$-1.09x10^{-5}$	$1.33x10^{-5}$	0.034
1174	$-2.95x10^{-5}$	$2.90x10^{-5}$	$-2.13x10^{-5}$	$1.81x10^{-5}$	0.020
1242	$-3.85x10^{-5}$	$4.59x10^{-5}$	$-2.25x10^{-5}$	$2.46x10^{-5}$	0.011
1315	$-4.29x10^{-5}$	$4.17x10^{-5}$	$-2.50x10^{-5}$	$1.81x10^{-5}$	0.004
1402	$-1.29x10^{-4}$	$1.12x10^{-4}$	$-6.73x10^{-5}$	$6.85x10^{-5}$	0.009
1439	$-3.94x10^{-5}$	$6.26x10^{-5}$	$-1.53x10^{-5}$	$1.56x10^{-5}$	0.003
1470	$-1.23x10^{-4}$	$7.40x10^{-5}$	$-7.13x10^{-5}$	$6.68x10^{-5}$	0.020
1516	$-1.35x10^{-4}$	$1.53x10^{-4}$	$-8.33x10^{-5}$	$5.56x10^{-5}$	0.018
1545	$-3.32x10^{-4}$	$3.21x10^{-4}$	$-1.63x10^{-4}$	$1.40x10^{-4}$	0.004
1657	$-5.08x10^{-4}$	$3.93x10^{-4}$	$-2.56x10^{-4}$	$1.93x10^{-4}$	0.002
2873	$-6.30x10^{-5}$	$5.17x10^{-5}$	$-4.30x10^{-5}$	$1.52x10^{-5}$	0.007
2961	$-9.23x10^{-5}$	$7.97x10^{-5}$	$-6.41x10^{-5}$	$2.99x10^{-5}$	0.015
3062	$-1.77x10^{-5}$	$9.21x10^{-6}$	$-1.41x10^{-5}$	$1.06x10^{-5}$	0.003
3074	$-1.69x10^{-5}$	$8.48x10^{-6}$	$-1.21x10^{-5}$	$9.92x10^{-6}$	0.004
3283	$-4.17x10^{-5}$	$3.26x10^{-5}$	$-3.09x10^{-5}$	$1.69x10^{-5}$	0.010
1034/837	$1.91x10^{0}$	$2.07x10^{0}$	$1.41x10^{0}$	$1.62x10^{0}$	0.043
772/1082	$1.21x10^{-1}$	$5.05x10^{-1}$	$-1.78x10^{-1}$	$2.89x10^{-1}$	**<0.001**
899/1082	$1.27x10^{-1}$	$5.59x10^{-1}$	$2.49x10^{-1}$	$3.92x10^{-1}$	0.032

1439/1402	$3.31x10^{-1}$	$1.87x10^{-1}$	$1.66x10^{-1}$	$2.13x10^{-1}$	0.019
1439/1516	$2.85x10^{-1}$	$1.09x10^{-1}$	$1.64x10^{-1}$	$1.41x10^{-1}$	0.003
1638/1516	$2.09x10^{0}$	$5.16x10^{-1}$	$2.21x10^{0}$	$1.12x10^{0}$	0.037
1439/1545	$1.23x10^{-1}$	$4.51x10^{-2}$	$8.94x10^{-2}$	$7.33x10^{-2}$	0.021
1455/1545	$3.67x10^{-1}$	$1.03x10^{-1}$	$3.82x10^{-1}$	$7.75x10^{-2}$	0.035
1470/1545	$3.44x10^{-1}$	$9.79x10^{-2}$	$3.84x10^{-1}$	$1.24x10^{-1}$	0.007
1638/1545	$8.85x10^{-1}$	$3.31x10^{-1}$	$1.05x10^{0}$	$6.98x10^{-1}$	0.013
1439/1657	$7.94x10^{-2}$	$3.19x10^{-2}$	$6.14x10^{-2}$	$4.77x10^{-2}$	0.026
1470/1657	$2.24x10^{-1}$	$6.33x10^{-2}$	$2.50x10^{-1}$	$8.72x10^{-2}$	0.005
1638/1657	$5.65x10^{-1}$	$2.91x10^{-1}$	$6.80x10^{-1}$	$6.73x10^{-1}$	0.011
2927/2852	$8.43x10^{-1}$	$1.58x10^{-1}$	$9.75x10^{-1}$	$2.77x10^{-1}$	0.002
2927/2873	$1.24x10^{0}$	$6.11x10^{-1}$	$1.60x10^{0}$	$8.37x10^{-1}$	0.001
2852/2927	$1.19x10^{0}$	$2.17x10^{-1}$	$1.03x10^{0}$	$2.72x10^{-1}$	0.002
2873/2927	$8.05\ x10^{-1}$	$3.50x10^{-1}$	$6.25x10^{-1}$	$2.50x10^{-1}$	0.001
2961/2927	$1.09x10^{0}$	$3.48x10^{-1}$	$7.79x10^{-1}$	$2.43x10^{-1}$	**<0.001**
3062/2927	$2.42x10^{-1}$	$1.53x10^{-1}$	$1.88x10^{-1}$	$1.59x10^{-1}$	0.026
2927/2961	$9.20x10^{-1}$	$2.95x10^{-1}$	$1.28x10^{0}$	$4.05x10^{-1}$	**<0.001**

TABLE IV. THE MEDIAN AND INTER-QUARTILE RANGE (IQR) OF BANDS OBTAINED FROM NORMALIZED AND SECOND DERIVATIVE OF THE WHOLE SERUM SPECTRA, AND THE P-VALUE WHEN COMPARING THESE BANDS BETWEEN THE PATIENT GROUPS. ONLY BANDS WITH A P-VALUE < 0.05 ARE PRESENTED.

	Discharged		Deceased		
Bands (cm^{-1})	Median	IQR	Median	IQR	*p*-value
828	$-3.56x10^{-4}$	$6.03x10^{-3}$	$7.22x10^{-3}$	$1.35x10^{-2}$	**<0.001**
898	$-1.00x10^{-3}$	$5.94x10^{-3}$	$-5.30x10^{-3}$	$5.52x10^{-3}$	0.003
1037	$-4.80x10^{-3}$	$6.27x10^{-3}$	$-8.10x10^{-3}$	$9.66x10^{-3}$	0.016
1657	$-1.44x10^{-1}$	$3.56x10^{-2}$	$-1.27x10^{-1}$	$4.16x10^{-2}$	0.014
2793	$-2.00x10^{-5}$	$2.59x10^{-3}$	$6.70x10^{-4}$	$2.53x10^{-3}$	0.016
2840	$1.62x10^{-2}$	$6.68x10^{-3}$	$1.84x10^{-2}$	$1.02x10^{-2}$	0.045
2854	$-2.63x10^{-2}$	$1.43x10^{-2}$	$-3.31x10^{-2}$	$2.75x10^{-2}$	0.023
1037/1320	$3.79x10^{-1}$	$5.63x10^{-1}$	$6.68x10^{-1}$	$7.62x10^{-1}$	0.011
1750/1320	$5.67x10^{-1}$	$9.28x10^{-3}$	$9.43x10^{-1}$	$1.40x10^{0}$	0.041
2793/1320	$1.71x10^{-3}$	$2.11x10^{-1}$	$-6.37x10^{-2}$	$2.49x10^{-1}$	0.014
1037/1547	$4.51x10^{-2}$	$6.45x10^{-2}$	$8.45x10^{-2}$	$1.25x10^{-1}$	0.009
1404/1547	$3.69x10^{-1}$	$5.72x10^{-2}$	$4.06x10^{-1}$	$1.10x10^{-1}$	0.013
TABLE IV. CONTINUATION.					
1431/1547	$-3.41x10^{-1}$	$5.15x10^{-2}$	$-3.71x10^{-1}$	$1.07x10^{-1}$	0.022
1657/1547	$1.53x10^{0}$	$1.31x10^{-1}$	$1.43x10^{0}$	$1.34x10^{-1}$	0.009
1750/1547	$6.93x10^{-2}$	$1.06x10^{-1}$	$1.39x10^{-1}$	$1.39x10^{-1}$	0.014
2793/1547	$2.00x10^{-4}$	$2.55x10^{-2}$	$-7.20x10^{-3}$	$2.96x10^{-2}$	0.016
2840/1547	$-1.72x10^{-1}$	$4.28x10^{-2}$	$-2.16x10^{-1}$	$9.54x10^{-2}$	0.001
2854/1547	$3.06x10^{-1}$	$1.01x10^{-1}$	$4.67x10^{-1}$	$2.86x10^{-1}$	0.005
2946/1547	$-3.16x10^{-1}$	$5.58x10^{-2}$	$-3.84x10^{-1}$	$8.77x10^{-2}$	**<0.001**
1037/1657	$3.01x10^{-1}$	$4.36x10^{-2}$	$6.55x10^{-2}$	$8.98x10^{-2}$	0.005
1404/1657	$2.45x10^{-1}$	$4.19x10^{-2}$	$2.83x10^{-1}$	$1.05x10^{-1}$	0.008
1431/1657	$-2.24x10^{-1}$	$3.42x10^{-2}$	$-2.57x10^{-1}$	$1.08x10^{-1}$	0.006
1547/1657	$6.53x10^{-1}$	$5.71x10^{-2}$	$6.97x10^{-2}$	$6.41x10^{-2}$	0.009
1639/1657	$5.60x10^{-1}$	$3.21x10^{-1}$	$6.58x10^{-1}$	$6.31x10^{-1}$	0.048
1750/1657	$4.99x10^{-2}$	$6.75x10^{-2}$	$8.80x10^{-2}$	$1.08x10^{-1}$	0.013
2793/1657	$1.40x10^{-4}$	$1.72x10^{-2}$	$-5.43x10^{-3}$	$2.02x10^{-2}$	0.018
2840/1657	$-1.15x10^{-1}$	$2.92x10^{-2}$	$-1.55x10^{-1}$	$4.45x10^{-2}$	**<0.001**
2854/1657	$2.07x10^{-1}$	$5.46x10^{-2}$	$3.12x10^{-1}$	$1.78x10^{-1}$	**<0.001**
2946/1657	$-2.06x10^{-1}$	$4.30x10^{-2}$	$-2.63x10^{-1}$	$6.97x10^{-2}$	**<0.001**
1173/2854	$4.35x10^{-1}$	$2.33x10^{-1}$	$2.98x10^{-1}$	$2.04x10^{-1}$	0.004
1517/2854	$1.42x10^{0}$	$7.56x10^{-1}$	$1.06x10^{0}$	$6.48x10^{-1}$	0.017
1547/2854	$3.26x10^{0}$	$1.15x10^{0}$	$2.14x10^{0}$	$1.96x10^{0}$	0.005
1657/2854	$4.83x10^{0}$	$1.41x10^{0}$	$3.22x10^{0}$	$2.36x10^{0}$	**<0.001**
1700/2854	$-2.48x10^{0}$	$1.01x10^{0}$	$-1.48x10^{0}$	$1.03x10^{0}$	0.005
2793/2854	$8.20x10^{-4}$	$1.09x10^{-1}$	$-2.36x10^{-2}$	$6.62x10^{-2}$	0.016

SVM and PCA-LDA predictive models were also developed based on the serum whole molecular composition spectra (**Table V**). As expected, normalized second derivate spectra preprocessing resulted in the highest accuracies, with PCA-LDA achieving 81%.

TABLE V. ACCURACY OF THE DEVELOPED PREDICTING MODELS, DEPENDING ON THE SPECTRA PREPROCESSING METHOD.

Preprocessing	Method	Others	Accuracy (%)
BC+UN*	SVM		63
	LDA	4PC's	71
2D*	SVM		58
	LDA	4PC's	77
2D+UN*	SVM		69
	LDA	4PC's	81

Abbreviations: * BC: Baseline Correction; 2D: Second Derivative; UN: Unit Vector Normalization; SVM: Support Vector Machines; LDA: Linear Discriminant Analysis; PC: Principal Component

B. Serum metabolome

Figure 4A represents the spectra of serum metabolome after baseline correction and unit vector normalization, while Figure 4B represents the averaged spectra of each patient group. These average spectra show slight differences, and consequently, the PCA score plot (**Fig. 4C**) enabled, partially, separation between the two groups.

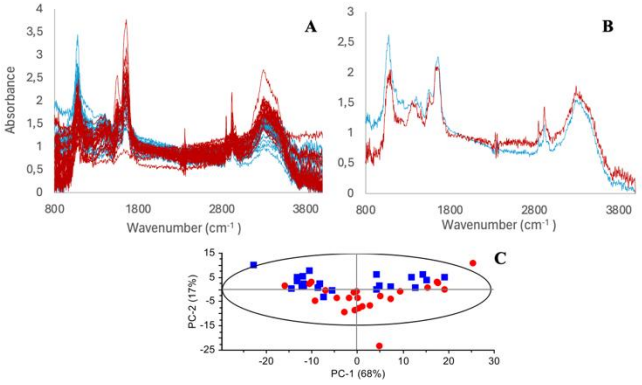

Fig. 4. Serum metabolome spectra after baseline correction and normalization of discharged (blue) and deceased (red) patients **(A)**. Corresponding averaged spectra **(B)** and PCA **(C)**.

The second derivative significantly increased the differences between the two groups (**Fig. 5A**) however, it reduced the separation in the PCA score plot (**Fig. 5B**).

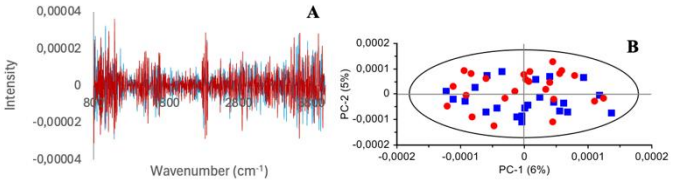

Fig. 5. Second derivative of serum metabolome average spectra of discharged (blue) and deceased (red) patients **(A)**, and corresponding PCA **(B)**.

By applying unit vector normalization to the second derivative spectra, a common scale was established (**Fig. 6A**). However, the PCA score plot (**Fig. 6B**) still did not show a clear separation between groups.

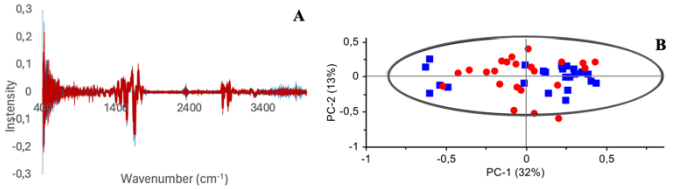

Fig. 6. Second derivative with unit vector normalization of serum metabolome spectra, of discharged (blue) and deceased (red) patients **(A),** and corresponding PCA **(B)**.

The major bands pointed in the normalized baseline-corrected spectra were analyzed. From the 14 bands and 56 ratios of bands analyzed, 42 were statistically different between the two groups (**Table VI**). The bands that were the most significantly different between the two groups, were 1074 cm^{-1}, 1156 cm^{-1}, 3299 cm^{-1} and 3366 cm^{-1} associated to phospholipids carbohydrates and amide A, respectively. The most significant ratios between bands included phospholipids (1236 cm^{-1}) and amide II (1555 cm^{-1}) and lipids (2909 cm^{-1}).

The same analysis based on the second derivative spectra, resulted in a smaller number of bands and ratios between bands (n=13), statistically different, between the two groups (**Table VII**), although a much higher number of bands and ratios were analyzed (n=275), mostly due to resolution of overlapped bands. The most significantly different bands between groups were 2851 cm^{-1} and 2917 cm^{-1} associated to lipids.

The analysis on the normalized second derivate spectra resulted in 34 bands and ratios statistically different, between the two groups of patients (**Table VII**), but with a much smaller number of bands analyzed (n=100). The band that was most significantly different between groups, was 1035 cm^{-1} associated to glycogen. The most significant ratios included amide III (1401 cm^{-1}) and amide II (1544 cm^{-1}) and amide I (1657 cm^{-1}).

TABLE VI. THE MEDIAN AND INTER-QUARTILE RANGE (IQR) OF BANDS OBTAINED FROM NORMALIZED AND BASELINE CORRECTED SERUM METABOLOME SPECTRA, AND THE P-VALUE WHEN COMPARING THESE BANDS BETWEEN THE PATIENT GROUPS. ONLY BANDS WITH A P-VALUE < 0.05 ARE PRESENTED.

	Discharged		Deceased		
Bands (cm^{-1})	Median	IQR	Median	IQR	*p*-value
1074	2.453	0.504	1.804	0.430	<**0.001**
1156	1.558	0.455	1.200	0.271	<**0.001**
1236	1.411	0.362	1.143	0.299	0.003
1250	1.318	0.381	1.180	0.242	0.009
TABLE VI. CONTINUATION.					
3299	1.522	0.227	1.780	0.301	<**0.001**
3366	1.381	0.203	1.637	0.229	<**0.001**
1236/1074	0.581	0.103	0.625	0.135	0.014
1250/1074	0.581	0.120	0.626	0.164	0.004
1402/1074	0.612	0.187	0.809	0.202	<**0.001**
1457/1074	0.578	0.130	0.751	0.146	<**0.001**
1555/1074	0.665	0.147	0.911	0.254	<**0.001**
1657/1074	0.910	0.183	1.347	0.282	<**0.001**
1074/1236	1.721	0.310	1.601	0.310	0.014
1156/1236	1.092	0.066	1.054	0.076	0.017
1250/1236	0.987	0.041	0.995	0.058	0.058
1402/1236	1.039	0.144	1.252	0.227	<**0.001**
1457/1236	0.975	0.112	1.192	0.221	<**0.001**
1555/1236	1.174	0.127	1.419	0.334	<**0.001**
1657/1236	1.570	0.344	2.132	0.527	<**0.001**
1074/1402	1.635	0.500	1.236	0.313	<**0.001**
1156/1402	1.079	0.209	0.863	0.149	<**0.001**
1236/1402	0.963	0.127	0.799	0.152	<**0.001**
1250/1402	0.957	0.111	0.814	0.124	<**0.001**
1657/1402	1.524	0.233	1.630	0.202	0.011
1074/1555	1.504	0.320	1.098	0.298	<**0.001**
1156/1555	0.954	0.154	0.723	0.159	<**0.001**
1236/1555	0.852	0.092	0.705	0.159	<**0.001**
1250/1555	0.851	0.123	0.697	0.167	<**0.001**
1657/1555	1.353	0.061	1.432	0.152	0.017
1074/1657	1.099	0.212	0.742	0.166	<**0.001**
1156/1657	0.696	0.174	0.505	0.151	<**0.001**
1236/1657	0.637	0.135	0.469	0.126	<**0.001**
1250/1657	0.621	0.135	0.495	0.120	<**0.001**
1402/1657	0.656	0.104	0.613	0.075	0.011
1457/1657	0.637	0.101	0.576	0.091	0.025
1555/1657	0.739	0.034	0.699	0.078	0.017
3299/2909	1.417	0.313	1.612	0.309	0.001
3366/2909	1.290	0.230	1.489	0.316	<**0.001**
2343/3299	0.507	0.197	0.418	0.159	0.003
3352/3299	0.509	0.164	0.430	0.170	0.009
2842/3299	0.632	0.165	0.527	0.075	0.006
2909/3299	0.706	0.156	0.620	0.120	0.001

TABLE VII. MEDIAN AND INTER-QUARTILE RANGE (IQR) OF BANDS OBTAINED FROM SECOND DERIVATIVE SERUM METABOLOME SPECTRA, AND THE P-VALUE WHEN COMPARING THESE BANDS BETWEEN THE PATIENT GROUPS. ONLY BANDS WITH A P-VALUE < 0.05 ARE PRESENTED.

	Discharged		Deceased		
Bands (cm^{-1})	Median	IQR	Median	IQR	*p*-value
820	$-1.70x10^{-5}$	$5.95x10^{-6}$	$-6.91x10^{-6}$	$1.38x10^{-5}$	0.009
849	$-1.13x10^{-5}$	$5.53x10^{-6}$	$-2.04x10^{-5}$	$1.75x10^{-5}$	0.013
1114	$-3.73x10^{-6}$	$8.68x10^{-6}$	$-9.27x10^{-6}$	$1.42x10^{-5}$	0.011
2851	$-2.72x10^{-5}$	$6.01x10^{-6}$	$-1.88x10^{-5}$	$6.72x10^{-6}$	<**0.001**
2917	$-2.31x10^{-5}$	$2.84x10^{-6}$	$-1.74x10^{-5}$	$7.54x10^{-6}$	<**0.001**
1114/849	$4.00x10^{-1}$	$3.02x10^{-1}$	$4.94x10^{-1}$	$1.25x10^{0}$	0.110
836/959	$1.01x10^{-1}$	$1.56x10^{0}$	$7.10x10^{-1}$	$2.41x10^{0}$	0.035
1114/959	$3.31x10^{-1}$	$4.36x10^{-1}$	$9.75x10^{-1}$	$2.40x10^{0}$	0.002
1641/1658	$1.97x10^{-1}$	$3.34x10^{-1}$	$-9.80x10^{-4}$	$5.34x10^{-1}$	0.048
1641/1697	$6.70x10^{-1}$	$5.06x10^{-1}$	$-1.03x10^{-1}$	$6.50x10^{-1}$	0.013
3103/2851	$3.11x10^{-1}$	$2.16x10^{-1}$	$4.97x10^{-1}$	$2.54x10^{-1}$	0.023
3005/2917	$1.04x10^{-1}$	$1.88x10^{-1}$	$2.08x10^{-1}$	$2.58x10^{-1}$	0.053
3103/2917	$3.06x10^{-1}$	$1.25x10^{-1}$	$5.09x10^{-1}$	$2.74x10^{-1}$	0.002

TABLE VIII. MEDIAN AND INTER-QUARTILE RANGE (IQR) OF BANDS OBTAINED FROM NORMALIZED AND SECOND DERIVATIVE SERUM METABOLOME SPECTRA, AND THE P-VALUE WHEN COMPARING THESE BANDS BETWEEN THE PATIENTS' GROUPS THAT THAT DECEASED OR WERE DISCHARGED FROM THE ICU. ONLY BANDS WITH A P-VALUE < 0.05 ARE PRESENTED.

	Discharged		Deceased		
Bands(cm^{-1})	Median	IQR	Median	IQR	*p*-value
837	$-4.71\ x10^{-3}$	$5.55\ x10^{-3}$	$-1.60\ x10^{-2}$	$1.74\ x10^{-2}$	0.003
1035	$-8.51\ x10^{-3}$	$5.49\ x10^{-3}$	$-1.20\ x10^{-2}$	$1.23\ x10^{-2}$	<**0.001**
1080	$-1.36\ x10^{-2}$	$4.74\ x10^{-3}$	$-2.81\ x10^{-2}$	$1.71\ x10^{-2}$	0.002
1544	$-9.82\ x10^{-2}$	$2.40\ x10^{-2}$	$-8.45\ x10^{-2}$	$2.17\ x10^{-2}$	0.006
TABLE VIII. CONTINUATION.					
1657	$-1.41\ x10^{-1}$	$3.09\ x10^{-2}$	$-1.22\ x10^{-1}$	$4.12\ x10^{-2}$	0.008
2927	$-2.70\ x10^{-2}$	$1.64\ x10^{-2}$	$-3.51\ x10^{-2}$	$1.85\ x10^{-2}$	0.002
837/1401	$1.19\ x10^{-1}$	$1.65\ x10^{-1}$	$4.46\ x10^{-1}$	$3.56\ x10^{-1}$	<**0.001**
1035/1401	$2.07\ x10^{-1}$	$1.19\ x10^{-1}$	$3.30\ x10^{-1}$	$4.04\ x10^{-1}$	<**0.001**
1080/1401	$3.69\ x10^{-1}$	$1.11\ x10^{-1}$	$6.30\ x10^{-1}$	$3.74\ x10^{-1}$	<**0.001**
1170/1401	$3.51\ x10^{-1}$	$6.71\ x10^{-2}$	$3.06\ x10^{-1}$	$9.01\ x10^{-2}$	0.026
2927/1401	$6.67\ x10^{-1}$	$3.15\ x10^{-1}$	$9.56\ x10^{-1}$	$6.01\ x10^{-1}$	<**0.001**
2964/1401	$6.34\ x10^{-1}$	$1.64\ x10^{-1}$	$6.99\ x10^{-1}$	$3.45\ x10^{-1}$	0.021
837/1544	$4.40\ x10^{-2}$	$6.12\ x10^{-2}$	$2.08\ x10^{-1}$	$1.92\ x10^{-1}$	<**0.001**
1035/1544	$8.24\ x10^{-2}$	$5.53\ x10^{-2}$	$1.35\ x10^{-1}$	$1.65\ x10^{-1}$	<**0.001**
1080/1544	$1.49\ x10^{-1}$	$4.89\ x10^{-2}$	$2.78\ x10^{-1}$	$1.98\ x10^{-1}$	<**0.001**
1235/1544	$1.08\ x10^{-1}$	$4.34\ x10^{-2}$	$1.22\ x10^{-1}$	$4.83\ x10^{-2}$	0.023
1457/1544	$3.33\ x10^{-1}$	$1.06\ x10^{-1}$	$4.07\ x10^{-1}$	$1.04\ x10^{-1}$	0.004
1470/1544	$3.48\ x10^{-1}$	$1.06\ x10^{-1}$	$3.99\ x10^{-1}$	$1.16\ x10^{-1}$	0.004
1517/1544	$4.68\ x10^{-1}$	$9.38\ x10^{-2}$	$5.16\ x10^{-1}$	$9.44\ x10^{-2}$	0.023
2927/1544	$2.69\ x10^{-1}$	$7.64\ x10^{-2}$	$4.64\ x10^{-1}$	$2.33\ x10^{-1}$	<**0.001**
2964/1544	$2.62\ x10^{-1}$	$6.66\ x10^{-2}$	$3.09\ x10^{-1}$	$9.69\ x10^{-2}$	<**0.001**
837/1640	$6.86\ x10^{-2}$	$7.99\ x10^{-2}$	$1.58\ x10^{-1}$	$1.83\ x10^{-1}$	0.013
1035/1640	$8.15\ x10^{-2}$	$8.19\ x10^{-2}$	$1.69\ x10^{-1}$	$1.11\ x10^{-1}$	<**0.001**
1080/1640	$1.67\ x10^{-1}$	$1.41\ x10^{-1}$	$2.59\ x10^{-1}$	$1.90\ x10^{-1}$	0.009
1170/1640	$1.60\ x10^{-1}$	$1.20\ x10^{-1}$	$1.05\ x10^{-1}$	$6.29\ x10^{-2}$	0.023
2927/1640	$2.99\ x10^{-1}$	$1.75\ x10^{-1}$	$4.56\ x10^{-1}$	$2.21\ x10^{-1}$	0.027
837/1657	$2.89\ x10^{-2}$	$3.95\ x10^{-2}$	$1.36\ x10^{-1}$	$1.46\ x10^{-1}$	0.001
1035/1657	$5.41\ x10^{-2}$	$3.82\ x10^{-2}$	$8.5\ x10^{-2}$	$1.16\ x10^{-1}$	<**0.001**
1080/1657	$9.27\ x10^{-2}$	$3.90\ x10^{-2}$	$1.81\ x10^{-1}$	$1.81\ x10^{-1}$	0.001
1457/1657	$2.26\ x10^{-1}$	$7.84\ x10^{-2}$	$2.52\ x10^{-1}$	$1.21\ x10^{-1}$	0.019
1470/1657	$2.24\ x10^{-1}$	$6.33\ x10^{-2}$	$2.50\ x10^{-1}$	$8.72\ x10^{-2}$	0.005

2850/1657	1.51 x10^{-1}	5.10 x10^{-2}	1.89 x10^{-1}	1.14 x10^{-1}	0.032
2927/1657	1.80 x10^{-1}	5.86 x10^{-2}	2.78 x10^{-1}	1.30 x10^{-1}	**<0.001**
2964/1657	1.66 x10^{-1}	6.38 x10^{-2}	2.01 x10^{-1}	6.44 x10^{-2}	**<0.001**

SVM and PCA-LDA predictive models were also developed based on the serum metabolome spectra (**Table IX**). The PCA-LDA generated the highest accuracy (93.61), for the normalized and baseline corrected spectra.

Table IX. Accuracy of the developed predicting models, according to the spectra preprocessing method.

Preprocessing	Method	Others	Accuracy (%)
BC+UN	SVM		70
	LDA	4PC's	94
2D	SVM		55
	LDA	4PC's	89
2D+UN	SVM		69
	LDA	4PC's	81

Abbreviations: * BC: Baseline Correction; 2D: Second Derivative; UN: Unit Vector Normalization; SVM: Support Vector Machines; LDA: Linear Discriminant Analysis; PC: Principal Component

The present study demonstrated that the serum metabolome captured the metabolic fingerprint associated with the patients' pathophysiological status more effectively than the whole serum, as indicated by the more accurate models obtained (94% vs. 81%). Since FTIR spectra of serum were acquired in a simple, cost-effective, and rapid manner, this method held potential as a cost-effective tool for predicting the pathophysiological state of critically ill patients.

ACKNOWLEDGMENT

This work was supported by the R-DICIP project (reference IPL/IDI&CA2024/R-DICIP_ISEL) granted by Instituto Politécnico de Lisboa (Portugal) and PREMO (reference DSAIPA/DS/0117/2020) granted by the Fundação para a Ciência e a Tecnologia (Portugal) (FCT). C. Rekowski, T. Fonseca, and R. Araújo, acknowledges the PhD grants from FCT, 2023.01951/BD, 2024.02043.BD and 2021.05553.BD, respectively.

REFERENCES

[1] Ahmed Z. (2022). Precision medicine with multi-omics strategies, deep phenotyping, and predictive analysis. *Progress in molecular biology and translational science*, *190*(1), 101–125. https://doi.org/10.1016/bs.pmbts.2022.02.002

[2] Zhao, J., Feng, Q., & Wei, W. Q. (2022). Integration of Omics and Phenotypic Data for Precision Medicine. *Methods in molecular biology (Clifton, N.J.)*, *2486*, 19–35. https://doi.org/10.1007/978-1-0716-2265-0_2

[3] R. Araújo, L.F.N. Bento, T.A.H. Fonseca, C.P. Von Rekowski, B. Ribeiro da Cunha, C.R.C Calado, "Infection Biomarkers Based on Metabolomics", Metabolites, 12(2), pp. 92, 2022. https://doi.org/10.3390/metabo12020092

[4] LM Ramalhete, R Araújo, A Ferreira, CRC Calado. Proteomics *for* Biomarker Discovery for Diagnosis and Prognosis of Kidney Transplantation Rejection. Proteomes. 2022*;* 10(3): 24. doi:10.3390/proteomes10030024. https://doi.org/10.3390/proteomes10030024

[5] T Fonseca, C Von Rekowski, R Araújo, MC Oliveira, G Justino, CRC Calado. The Impact of Serum extraction protocol on metabolomic profiling using UPLC-MS/MS and FTIR spectroscopy. ACS Omega. 2023; 8(23): 20755–20766. doi:10.1021/acsomega.3c01370 https://doi.org/10.1021/acsomega.3c01370

[6] Magalhães, S., Goodfellow, B. J., & Nunes, A. (2021). FTIR spectroscopy in biomedical research: how to get the most out of its potential. *Applied Spectroscopy Reviews*, *56*(8–10), 869–907. https://doi.org/10.1080/05704928.2021.1946822

[7] BR Cunha, SM Aleixo, LP Fonseca, CRC Calado. Fast identification of off-target liabilities in early antibiotic discovery with Fourier-transform infrared spectroscopy. Biotechnol Bioeng. 2021; 118 (11): 4465-4476. doi: 10.1002/bit.27915 https://doi.org/10.1002/bit.27915

[8] BR Cunha, LP Fonseca, CRC Calado. Simultaneous elucidation of antibiotics mechanism-of-action and potency with high-throughput fourier-transform Infrared spectroscopy and machine-learning. App Microb Biot. 2021; 105(3): 1269-1286. doi: 10.1007/s00253-021-11102-7. https://doi.org/10.1007/s00253-021-11102-7

I Correia holds a bachelor's degree in chemical and biological engineering (2023) from ISEL. She is currently a master's student in biomedical engineering and working on the FCT-approved PREMO project, with the ambition to pursue a PhD in biomedical engineering. https://orcid.org/0009-0007-5085-2542

T Fonseca holds a bachelor's degree in health sciences (2019) and a master's in biomedical engineering (2022) from ISEL. He is currently pursuing a Ph.D. in Biomedicine at Nova Medical School. Since 2020, he has been a research fellow at ISEL, working on the FCT-approved PREMO project. His research focuses on metabolomics and FTIR analysis, using blood serum samples from ICU patients. His primary goal is to identify biomarkers that can predict patient outcomes in critical care units, hence improving predictive models for morbidity and mortality. https://orcid.org/0000-0003-0741-2211

J Pataco holds a bachelor's degree in humam biology (2020) from Universidade de Évora and a master's in legal medicine and forensic sciences (2022) from Faculdade de Medicina da Universidade de Coimbra. She is currently a master's student in biomedical engineering at ISEL and working on the FCT-approved PREMO project. https://orcid.org/0000-0002-8531-314X

M. Oliveira has a degree in Biomedical Engineering (2024) from ISEL and is currently a master's student in the same area. She is involved in the PREMO project, approved by FCT, and intends to pursue her PhD after completing her master's degree.

V Caldeira has a master's degree in biomedical engineering, from Instituto Superior de Engenharia de Lisboa (ISEL). Currently, she is a PhD candidate in Biomedicine, at NOVA Medical School. Her research goes towards innovation and precision medicine, studying metabolomics to develop predictive models, with machine learning. She has been a researcher at the Laboratory of Engineering & Health, from ISEL' group, since 2017. Her background is related to in vitro research, cell culture and metabolomics using FTIR analysis.

N Domingues Nuno A. S. Domingues, PhD candidate in Education from ISPA+NOVA, Pós Doc in Information Science and Technology from ISCTE (2023), Pós Doc in Mechanical Engineering from IST (2022), Pós Doc in Science Communication from FCSH-UNL (2021), Pós Doc in Electrical Engineering and Computer Science from IST (2020), PhD in Electrical Engineering and Computer Science from FCT-UNL (2015), Master in Electrical Engineering and Computer Science from IST (2008), Undergraduate (5-year) in Electrical Engineering from ISEL (2005).His topics of research include modelling and simulation, energy systems and mobility, SCADA and DSS, decision making, e-learning, science communication, education. He is a Professor in ISEL Engineering Polytechnic University. He holds a Problem Based Learning and Excellence in Teaching and Learning diploma by UNESCO and the internationally Information Technology ECDL qualification. He has the Leadership certification by the Military Academy. He is a recognised science and engineer trainer by Conselho Científico-Pedagógico da Formação Contínua (Minho University). He is a Member of the Institute of Electrical and Electronics Engineers (IEEE). https://orcid.org/0000-0003-0763-8106

C Von Rekowski holds a degree in Clinical Physiology (2019) from Escola Superior de Tecnologia da Saúde de Lisboa and a master's in biomedical engineering (2022) from ISEL. She has been a research fellow at ISEL since 2020, working on an FCT-approved project focusing on biomarker identification, using metabolomics, proteomics, and machine learning. She is currently pursuing a Ph.D. in Biomedicine at Nova Medical School, while also supporting the work of various master's students. Her work focuses on building databases, performing statistical analysis of demographic, clinical, and laboratory data, and using this data to develop predictive models for morbidity and mortality in critically ill patients. https://orcid.org/0009-0009-6843-1935

R Araújo holds several engineering degrees (Mechanical, Biomedical). A researcher at the Laboratory of Engineering and Health (ISEL) since 2017, focusing on biomarkers through metabolomics and proteomics for applications in toxicology, pharmacology, and more. His current PhD research, part of an FCT-approved project, studies COVID-19 biomarkers in critically ill patients using machine learning. https://orcid.org/0000-0002-9369-6486

L Bento completed his PhD in Clinical Research in 2018, at *Universidade Nova de Lisboa | Faculdade de Ciências Médicas*, and his Medical degree in 1994, at the same institution. He is the Coordinator of the Medical Emergency Unit at *Centro Hospitalar Universitário Lisboa Central EPE*, Head of the Intensive Care Medicine Department, and a Consultant in Internal Medicine. He also serves as an Assistant Professor at *Universidade Nova de Lisboa* and is a specialist in Internal Medicine and Intensive Care Medicine. He has worked in areas such as acute-on-chronic liver failure, acute kidney injury, multi-organ failure, hepatic transplant, and hemodynamic instability, with a focus on intensive care and emergency medicine. https://orcid.org/0000-0002-0260-003X

CRC Calado is Coordinating professor with Aggregation at ISEL. She has a BSc in Biochemistry, an MSc and a PhD in Biotechnology and an Aggregation in Biochemistry. She is the coordinator of the BSC in Biomedical Engineering and the R&D Laboratory in Health & Engineering. Her research focuses on Bioprocess Engineering and Development of Platforms for Drugs and Biomarkers Discovery.
https://orcid.org/0000-0002-5264-9755